Anais da Academia Brasileira de Ciências (2017)
(Annals of the Brazilian Academy of Sciences)
Printed version ISSN 0001-3765 / Online version ISSN 1678-2690
http://dx.doi.org/10.1590/0001-3765201720170317
www.scielo.br/aabc | www.fb.com/aabcjournal

Generation of a triple-fluorescent mouse strain allows a dynamic and spatial visualization of different liver phagocytes *in vivo*

BRENDA N. NAKAGAKI[1], MARIA A. FREITAS-LOPES[1], ÉRIKA CARVALHO[1], RAQUEL CARVALHO-GONTIJO[1], HORTÊNCIA M. CASTRO-OLIVEIRA[1], RAFAEL M. REZENDE[2], DENISE C. CARA[1], MÔNICA M. SANTOS[3], RODRIGO PESTANA LOPES[4], BRUNA A. DAVID[1,5*] and GUSTAVO B. MENEZES[1*]

[1]Center for Gastrointestinal Biology, Departamento de Morfologia, sala N3-140, Instituto de Ciências Biológicas, Universidade Federal de Minas Gerais, Av. Presidente Antônio Carlos, 6627, Pampulha, 31270-901 Belo Horizonte, MG, Brazil
[2]Ann Romney Center for Neurologic Diseases, Department of Neurology, Brigham and Women's Hospital, Harvard Medical School, 60 Fenwood Road, 02115, Boston, MA, United States of America
[3]Departamento de Biologia Animal, Universidade Federal de Viçosa, Av. Peter Henry Rolfs, s/n, Campus Universitário, 36570-900 Viçosa, MG, Brazil
[4]BD Biosciences, Rua Alexandre Dumas, 1976, Chácara Santo Antônio, 04717-040 São Paulo, SP, Brazil
[5]Departamento de Bioquímica e Imunologia, Faculdade de Medicina de Ribeirão Preto, Universidade de São Paulo/USP, Av. Bandeirantes, 3900, Monte Alegre, 14049-900 Ribeirão Preto, SP, Brazil

Manuscript received on May 3, 2017; accepted for publication on June 28, 2017

ABSTRACT

Resident and circulating immune cells have been extensively studied due to their almost ubiquitous role in cell biology. Despite their classification under the "immune cell department", it is becoming increasingly clear that these cells are involved in many different non-immune related phenomena, including fetus development, vascular formation, memory, social behavior and many other phenotypes. There is a huge potential in combining high-throughput assays - including flow cytometry and gene analysis - with *in vivo* imaging. This can improve our knowledge in both basic and clinical cell biology, and accessing the expression of markers that are relevant in the context of both homeostasis and disease conditions might be instrumental. Here we describe how we generated a novel mouse strain that spontaneously express three different fluorescence markers under control of well-studied receptors (CX3CR1, CCR2 and CD11c) that are involved in a plethora of stages of cell ontogenesis, maturation, migration and behavior. Also, we assess the percentage of the expression and co-expression of each marker under homeostasis conditions, and how these cells behave when a local inflammation is induced in the liver applying a cutting-edge technology to image cells by confocal intravital microscopy.

Key words: intravital microscopy, phagocytes, liver immunology, fluorescent markers, hepatology, gastroenterology, immunology.

Correspondence to: Gustavo Batista de Menezes
E-mail: menezesgb@ufmg.br
*These authors jointly supervised this project.

** Contribution to the centenary of the Brazilian Academy of Sciences.

INTRODUCTION

A brilliant Russian zoologist named Ilya Ilyich Mechnikov in 1892 described the phagocytes (in special macrophages and neutrophils), and since then, these cells have amazed diverse researches by their ability to rapidly respond to insults and also to seed or infiltrate in almost all body tissues. Especially due to their fast moving capacity and mainly by their efficient role to engulf and destroy pathogens and foreign bodies, these cells have been extensively used in cell biology assays (Yipp et al. 2012, David et al. 2016). Interestingly, despite almost every single organ in the body has its own population of macrophages – which can actually be similar in morphology and shape between the organs - these cells have a sharp different function within the tissues. For example, while microglia are sessile and long living cells in the central nervous system and add to the maintenance of neuron homeostasis (Yona et al. 2013, Parkhurst et al. 2013), intestinal macrophages act as regulating cell to induce resistance to microorganisms, avoiding excess tissue damage and may be substituted during the life by infiltrating monocytes (Ginhoux and Jung 2014, Balmer et al. 2014).

It is well known that during embryogenesis macrophage precursors migrate from the yolk sac in the initial phases of embryo development to seed fetal tissues, mainly the brain or the primordial liver (Davies et al. 2013, Geissmann et al. 2010, Ginhoux and Jung 2014, Gomez Perdiguero et al. 2015, Yona et al. 2013). A second wave of macrophage population happens when these liver monocytes migrate from the fetal liver to the different organs to give rise to a very heterogeneous population of resident macrophages. Despite their different function, the contribution rate of self-renewing *versus* the migration of circulation monocytes to maintain the pool of these cells is particular to every tissue. For example, while skin macrophages are almost 100% substituted by a $Ly6G^{hi}$ circulating monocytic precursor during over the life, fetal liver-derived hepatic macrophages (usually refereed as Kupffer cells (KC)), are mostly self-renewed cells, and a minor contribution of bone-marrow derived monocytes is expected to renew the resident pool in steady state (Faust et al. 2000, Fogg et al. 2006, Ginhoux and Jung 2014). Therefore, such complexities in the different ontogenesis make the studies of different populations in macrophages very difficult, and probably confusing. This clearly shows that to properly generate reliable data in macrophage biology field, it might be necessary to combine different methods *in vivo* and *ex vivo.*

Several different cell subtypes, including dendritic cells, hepatic stellate cells (also known as Ito cells) and other leukocyte subtypes naturally inhabit the liver (Fig. 1). The liver homes the largest population of macrophages in the body, and the major part of these cells inhabit the intraluminal space, and together with the liver sinusoidal cells, they comprise the largest reticulo-endothelial system in the body (Crispe 2009). Kupffer cells may have several functions in the hepatic homeostasis. Under normal conditions, they induce a tolerogenic milieu in the liver to avoid unwanted immune response due to gut-derived antigens, and also remove aged red-blood cells and foreign bodies out of the circulation. Notably, these cells have the amazing ability to arrest circulating bacteria (David et al. 2016, Jenne and Kubes 2013, Thomson and Knolle 2010). The mechanisms involved in this particular "rapid catching behavior" under flow are still elusive, and hold interesting opportunity for future investigation.

Considering that the liver is interposed between the blood that arises form whole intestinal circulation (which is rich in bacterial products) and the systemic blood (which is free of pathogens in health), it is expected that liver reticulo-endothelial system exerts an infallible function in filtering the blood. This helps to avoid continuous hepatic inflammation and also bacterial spread within the

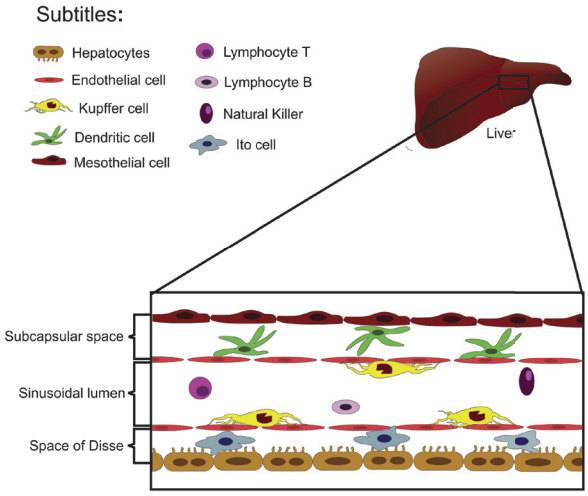

Figure 1 - Schematic representation of liver cell populations. In addition to the parenchymal cells, different immune cell subtypes inhabit the liver. Dendritic cells are mainly located underneath the liver capsule (mesothelial cells), while Stellate cells (also known as Ito cells) are in a narrow space separating the sinusoid from hepatocytes, called space of Disse. Macrophages are exclusively found lining the sinusoidal endothelium (also known as Kupffer cells) while in the lumen, there is a plethora of resident leukocytes, including lymphocytes, monocytes and eventual granulocytes.

body organs. Therefore, it is rational to postulate that different cells with phagocytic behavior would be distributed within the liver compartments to properly perform this task. However, the diversity of these cells, combined with the limitations of the conventional histology and digestion procedures that are necessary to characterize these cells using flow cytometry, have limited our understanding of their actual location, shape and manly function *in vivo*. Fortunately, novel techniques have allowed the visualization of these cells in their original territory in living small rodents and other species (i.e. *Drosophila melanogaster* and *Caenorhabditis elegans*) (Arkhipov et al. 2016, Karreman et al. 2016). This strategy is based in performing direct whole-organism imaging (in case of small species) or different surgical approaches to expose organs *in vivo* and image cells using a microscope. The advent of faster acquisition devices with laser scanning confocal heads have hugely improved our tools to visualize these cells *in vivo* in solid organs as spleen and the liver (where conventional illumination using regular white light has imposed limitations in imaging quality over the years). Also the option to use multi-color acquisition setups made possible identification of more complex populations *in vivo*, since several fluorescent receptors and markers can be superposed and distinct populations of phagocytes could be better characterized in their original location.

To enhance the available tools for these investigations, we selected three main cellular makers that are expressed in different phagocytes: the integrin CD11c (that are expressed in almost all macrophages and dendritic cells) (Lindquist et al. 2004), and two chemokine receptors that are key in the macrophage location and behavior (CCR2 and CX3CR1) (Mizutani et al. 2012) to generate a novel mouse strain that express simultaneously these different fluorescent proteins. The spontaneously expression of these three reporters facilitate *in vivo* investigation of their spatial location, dynamics and function using flow cytometry and confocal intravital microscopy (David et al. 2016, Marques et al. 2015, McDonald et al. 2010). Of note, since fluorescent probes are precluded to reach some of these cells within tissues, "spontaneously staining" by self-expressing proteins is instrumental. Here, we also demonstrated - exploring a combination of flow cytometry and intravital studies – that the liver has a very intricate population of immune cells, that are heterogeneously distributed within the liver compartments and behave differentially in the steady state and when the liver was challenged with a local challenge.

MATERIALS AND METHODS

ANIMALS

C57BL/6 wild type, CCR2$^{rfp/rfp,}$ CX3CR1$^{gfp/gfp}$ and CX3CR1$^{gpf/wt}$ and CD11c-EYFP mice were from Centro de Bioterismo in Universidade Federal

de Minas Gerais (CEBIO – UFMG, Brazil) or bred in our mice facility. All animals were housed in a conventional specific pathogen-free facility at the Universidade Federal de Minas Gerais according to the animal protocol with the full knowledge and permission of the Standing Committee on Animals at all institutions (CEUA 384/2016).

BREEDING STRATEGY

To generate a mouse strain that expresses three fluorescence molecules without delete their expression in both alleles ($CX3CR1^{gfp/wt}CCR2^{rfp/wt}$CD11c-eYFP), we made an extensive breeding protocol using 5 different mouse genotypes. First, we crossed CCR2 knockout mice that both CCR2 alleles were replaced by a RFP sequence ($CCR2^{rfp/rfp}$) with CX3CR1 knockout mice that the CX3CR1 alleles were knocked out and replaced by a GFP sequence ($CX3CR1^{gfp/gfp}$) The F1 offspring was 100% heterozygote for both receptors (here called as $CX3CR1^{gfp/wt}$ $CCR2^{rfp/wt}$) (Fig. 4a). To generate a double knockout colony $CX3CR1^{gfp/gfp}$ $CCR2^{rfp/rfp}$), we breed heterozygotes ($CX3CR1^{gfp/wt}$ $CCR2^{rfp/wt}$) (Fig. 4b). Finally, we bred this double homozygote strain with mice that have eYFP expression under control of CD11c, generating a triple heterozygote and triple fluorescence expressing strain $CX3CR1^{gfp/wt}CCR2^{rfp/wt}$CD11c-eYFP) (Fig. 4c).

INTRAVITAL CONFOCAL MICROSCOPY

Confocal intravital imaging was performed as described (David et al. 2017). In brief a midline laparotomy was performed followed by removal of the skin and abdominal muscle along the costal margin to the mid-axillary line to expose the liver. Mice were placed in the right lateral position and a single liver lobe was exteriorized on the custom-made Plexiglas microscope stage. All exposed tissues were moistened with saline-soaked tissue paper to prevent dehydration during imaging. For the duration of all experiments, body temperature was maintained with an infrared heat lamp, and the liver was continuously perfused with physiological phosphate-buffered buffer. After preparation for intravital and immediately prior to imaging, a single focal injury was induced on surface of the liver using the tip of a heated 30-guage needle mounted on an electro-cautery device. Necrotic cells were immediately labelled with a single application of 50 µL of 1 mM DAPI solution to the surface of the liver. Previously to surgery, fluorescence-expressing mice received a single dose or a mixture of the following antibodies or fluorescent probes: anti-Ly6G APC (4 µg, clone 1A8, BD Horizon, USA), anti-CD31 BV-421 (4 mg, clone MEC 13.3,), DAPI (0.1 ml at 1 mM, Sigma, USA). Mice were imaged using a Nikon Eclipse Ti with an A1R confocal microscope loaded with a spectral detector and XYZ motorized stage. Since eYFP and GFP have very close fluorescence spectra, we excited eYFP-expressing cells with 514nm laser and collected the signal from 566-578nm using the virtual filter function, and GFP-expressing cells were imaged using the same setup, but cells were excited with a 488nm laser and the signal was collected between a 488-506nm wavelength. Proper controls were made with only eYFP or GFP expressing tissues in order to calibrate our spectral separation protocol. Cell density, movies, location and 3D rendering were made using Volocity (6.3) Perkin Elmer, USA. For movies, three different fields were simultaneously acquired using the motorized programing of the microscope stage, and during 3 consecutive hours, images from all channels were acquired with an interval of 1 minute between the frames. We chose to image using a 20x objective an area in the center of the thermal injury, an area adjacent to the injury and a distant area from de injury. All movies were made under the same microscope setup and edited offline using iMovie (Apple, USA).

LIVER NON-PARENCHYMAL CELLS (LNPCS) ISOLATION

Liver non-parenchymal cells were isolated as previously reported (David et al. 2017). In brief, livers were digested in a collagenase solution and cells were differentially separated by centrifugation. Using an Accuri C6 cytometer (BD Biosciences), 1 x 10^6 cells were acquired using the following setup: all cells were excited by a 488nm laser, and GFP cells were acquired in FL1 channel loaded with a 510/15nm filter, YFP cells in FL2 channel using a 540/20nm filter and RFP cells were estimated using FL3 channel with a 610/20nm filter. Different gates for exclusion of cell debris, duplets and for estimation of the percentage of fluorescence expressing cells were made using FlowJo 10. All filters and reagents were a kind gift from BD Biosciences.

RESULTS

LIVER HAS A LARGE POPULATION OF IMMUNE CELLS THAT CAN BE DETECTED USING DIFFERENT FLUORESCENCE-EXPRESSING REPORTER MOUSE STRAINS

Our imaging platform is an adaptation of a stock Nikon Ti-E Inverted Microscope coupled with an A1R confocal head with a high-resolution Galvano scanner and high-sensitive photomultiplier tubes (PMTs), that allows for imaging resolution up to 4096 x 4096 pixels. By combining the scanner and the motorized Piezo Z stage, high-speed 3D scanning can be achieved for live imaging. Using the spectral imaging detector, up to 32 channels can be acquired simultaneously and fluorofores with very similar spectral fluorescence emission (i.e., eYFG and eGFP) can be adequately separated. Using a custom made acrylic stage, anesthetized mice can be positioned in the microscope imaging field after liver surgical approach, owing to intravital imaging acquisition (Fig. 2).

To image liver phagocyte spatial location, we used three mouse strains that express fluorescent proteins under control of target genes that are expressed by these cells under different conditions (Fig. 3a). Also, to geographically locate these cells within the liver tissue, we stained the sinusoidal endothelial cells with an intravenous injection of BV421-conjugated anti-CD31 (anti-PECAM-1; BD Biosciences) (Fig. 3b). This same strategy was used throughout all imaging protocols. Using a mouse strain that express red fluorescent protein under control of the chemokine-receptor CCR2 ($CCR2^{rfp/wt}$, here shown in white for illustration purpose), we observed that the liver has a vast population of CCR2+ cells that distributed throughout the whole imaging field, and are located in both intravascular and extravascular compartments. Some of these cells have a round shape and this subpopulation was seen mostly inside the sinusoidal lumen, suggesting that they may comprise a population of infiltrating CCR2+ monocytes and neutrophils. However, some of star-shaped CCR2+ cells were observed in the extravascular space, mainly underneath the liver mesothelium layer (subcapsular space), which suggests a population of CCR2-expressing dendritic cells (Fig. 3a and b). In fact, a very similar landscape was imaged when we used a mouse strain that express the enhanced-yellow fluorescent protein (e-YFP; here shown in red for illustration purpose) under control of the b2-integrin CD11c (also known as integrin alpha X, complement component 3 receptor 4 subunit or ITGAX). In this case, the YFP was placed under the transcriptional control of the CD11c promoter without knocking out its expression. In these mice, we could also detect a large population of subcapsular CD11c+ cells, but also an intravascular population of sessile star-shaped cells, suggesting that the extravascular cells may be a population of liver dendritic cells, while the intraluminal cells are a subpopulation of CD11c-expressing Kupffer cells. However, when we used a mouse strain expressing green-fluorescent protein (GFP) under control of the fracktalkine receptor CX3CR1 ($CX3CR1^{gfp/wt}$,

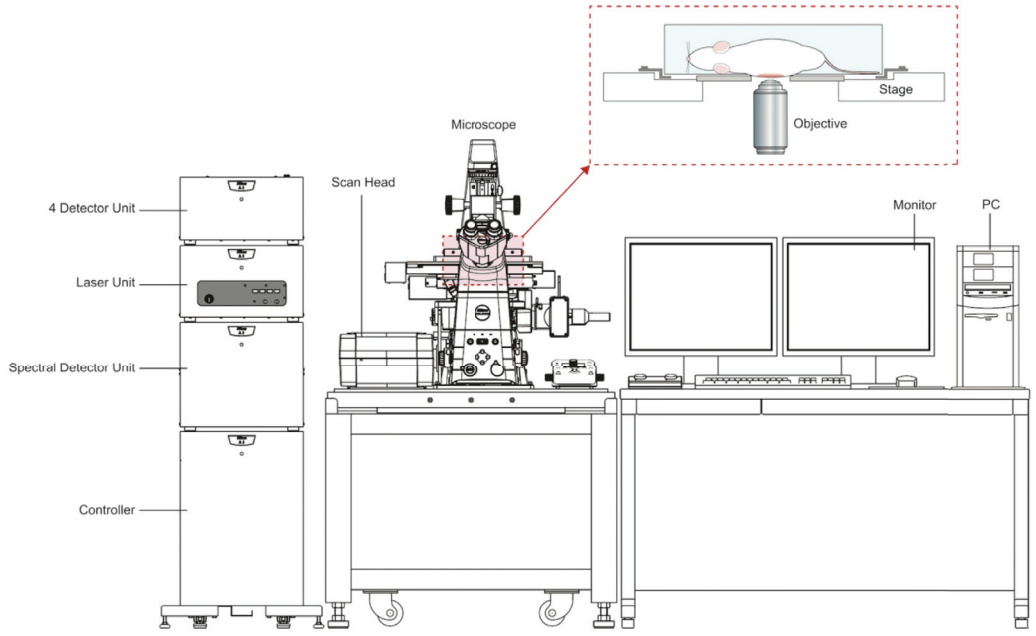

Figure 2 - Schematic representation of microscope setup for confocal intravital microscopy. After the surgical procedure, mouse is positioned on an acrylic stage over the microscope objective for image and/or video acquisition (enlarged detail of the dashed frame). Images were made in a Nikon A1R confocal microscope.

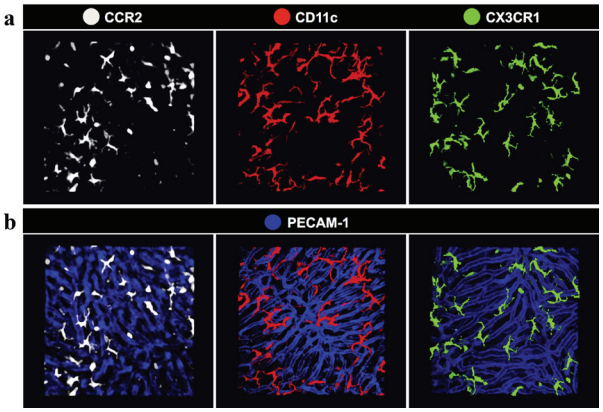

Figure 3 - Three-dimensional rendering of liver phagocytes of different mouse strains. (**a**) Liver confocal intravital microscopy imaging through the capsule evidencing the distribution of CCR2$^{rfp/wt}$ (white), CD11c-YFP (red) and CX3CR1$^{gfp/wt}$ (green) mice, respectively. (**b**) Image merged with PECAM-1 to geographically locate these cells within the liver tissue.

also known as G-protein coupled receptor 13, GPR13), we revealed an exclusively dendritic-shaped extravascular cell population, that was not seen inside the sinusoidal lumen. These cells were previously identified of a population of liver dendritic cells (David et al, 2016). Eventual round CX3CR1+ cells were seen patrolling the vessels, which we considered as circulating monocytes.

GENERATION OF A TRIPLE FLUORESCENT MOUSE ALLOWS THE IDENTIFICATION OF SUBPOPULATIONS OF LIVER PHAGOCYTES THAT CAN CO-EXPRESS MULTIPLE FLUORESCENT MARKERS

Our previous data using single-fluorescence expressing mouse strains revealed that some hepatic immune cell subpopulations that report different molecules are very similar in shape, distribution and location. This suggests that a single phagocyte population can express simultaneously several markers. To dissect these different populations, we generated a novel mouse strain that spontaneously reports the expression of CD11c, CX3CR1 and CCR2 under baseline conditions. To achieve this phenotype, as described in details methods, we bred a CCR2 knockout mouse that had both CCR2 alleles replaced by an RFP gene sequence

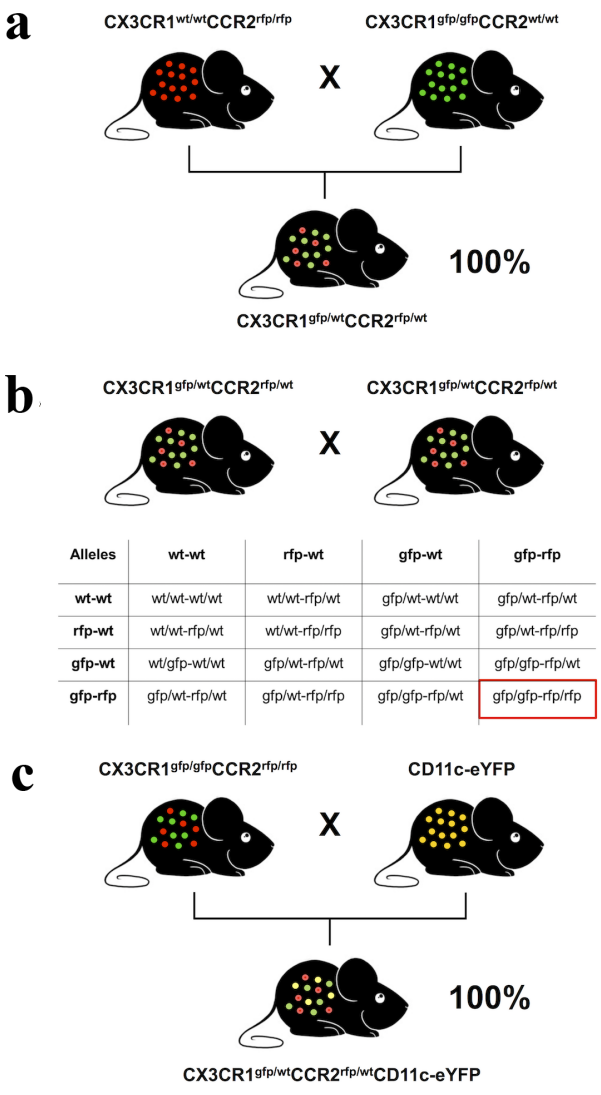

Alleles	wt-wt	rfp-wt	gfp-wt	gfp-rfp
wt-wt	wt/wt-wt/wt	wt/wt-rfp/wt	gfp/wt-wt/wt	gfp/wt-rfp/wt
rfp-wt	wt/wt-rfp/wt	wt/wt-rfp/rfp	gfp/wt-rfp/wt	gfp/wt-rfp/rfp
gfp-wt	wt/gfp-wt/wt	gfp/wt-rfp/wt	gfp/gfp-wt/wt	gfp/gfp-rfp/wt
gfp-rfp	gfp/wt-rfp/wt	gfp/wt-rfp/rfp	gfp/gfp-rfp/wt	gfp/gfp-rfp/rfp

Figure 4 - Breeding strategy to generate a triple fluorescence strain. (**a**) CCR2 knockout mice that both CCR2 alleles were replaced by an RFP sequence ($CCR2^{rfp/rfp}$) were bred with CX3CR1 knockout mice which CX3CR1 alleles were knocked out and replaced by a GFP sequence ($CX3CR1^{gfp/gfp}$). The F1 offspring was 100% heterozygote for both receptors ($CX3CR1^{gfp/wt}$ $CCR2^{rfp/wt}$). (**b**) To further generate double-knockout mice ($CX3CR1^{gfp/gfp}$ $CCR2^{rfp/rfp}$), heterozygous mice for CX3CR1 and CCR2 (F1) were bred. Possible genotypes of the offspring of this breeding were illustrated by the allelic combination of F1 animals showing a ratio of 1/16 of double-knockout mice (F2). (**c**) To generate a mouse with triple fluorescence, F2 double-knockout mice ($CX3CR1^{gfp/gfp}$ $CCR2^{rfp/rfp}$) bred with mice expressing e-YFP under control of CD11c. Then, were reached a 100% progeny of heterozygous mice for the three receptors (CX3CR1, CCR2 and CD11c) and triple fluorescence (GFP, RFP and YFP, respectively).

($CCR2^{rfp/rfp}$) with another mouse strain that the CX3CR1 alleles were knocked out and substituted by GFP ($CX3CR1^{gfp/gfp}$). The F1 offspring was 100% heterozygote for both genes, which means that now all pups are now $CX3CR1^{gfp/wt}$ $CCR2^{rfp/wt}$. These mice were healthy and had normal development and fertility. Next, we breed these two heterozygote strains until we reached a double homozygote offspring for CX3CR1 and CCR2 ($CX3CR1^{gfp/gfp}CCR2^{rfp/rfp}$). Of note, these mice were deficient for both CX3CR1 and CCR2 receptors; however, we could not detect any susceptibility for diseases or breeding issues. Finally, we bred the double homozygote $CX3CR1^{gfp/gfp}CCR2^{rfp/rfp}$ with the CD11c-eYFP mouse to reach a F1 offspring that all pups were $CX3CR1^{gfp/wt}CCR2^{rfp/wt}$CD11c-eYFP. To confirm that our breeding strategy was successful, we isolated liver non-parenchymal cells and investigated subpopulations using flow cytometry. Custom made filters were used to allow the detection and efficient separation of these three fluorescent proteins. As shown in Fig. 5a and b, $CX3CR1^{gfp/wt}CCR2^{rfp/wt}$CD11c-eYFP mouse had all these 3 subpopulations within liver non-parenchymal cells. In line with our intravital data, flow cytometry confirmed that liver has a mixed population that might have none of these receptors, but may express one or two simultaneous reporters, revealing the complexities of hepatic immune cell populations and the diverse expression of different cell markers.

SPECTRAL IN VIVO SEPARATION OF FLUORESCENCE CONFIRMS THE PRESENCE AND SPATIAL DISTRIBUTION OF MULTI-FLUORESCENCE EXPRESSING POPULATIONS

Cell isolation from organs to further flow cytometry studies is a widely used methodology to characterize cell populations with different organs in high-dimensional way, and this has enormously enhanced our understanding of the immune response under different circumstances in homeostasis

and disease. However, in order to specifically illuminate a single cell in the flow chamber inside the cytometer, cells need to be removed out of their *in vivo* context and prepared in a diluted solution. Therefore, despite the advantages of multiple staining with different antibodies, cell separation procedures have a digestion step that dissolves the organ, losing geographical location and possibly also altering cell shape and morphology. For superseding these limitations, we imaged all these liver phagocytes using a spectral detector coupled in a confocal microscope that allowed the identification of all fluorescence-expressing cells in CX3CR1$^{gfp/wt}$CCR2$^{rfp/wt}$CD11c-eYFP mouse in their native habitat. As shown in Fig. 6a, our spectral separation efficiently separated all 3 different populations, depicted here in white (CCR2+ cells), red (CD11c+ cells) and green (CX3CR1+ cells). Strikingly, when we merged channels, we could detect that some CD11c+ cells are also CX3CR1+ (shown as yellowish cells) (Fig. 6b). Using the hepatic microvasculature as a spatial reference (stained in blue by anti-PECAM-1), we precisely compartmentalized several populations that were or intravascularly located (mainly a population of CD11c+CCR2+ cells) or a large population that inhabited the subcapsular environment (mostly CX3CR1+CD11c+ or triple positive cells) (Fig. 6b). Taking together, these data revealed how complex and diverse is the liver population of immune cells using a combination of an *ex* and *in vivo* approach.

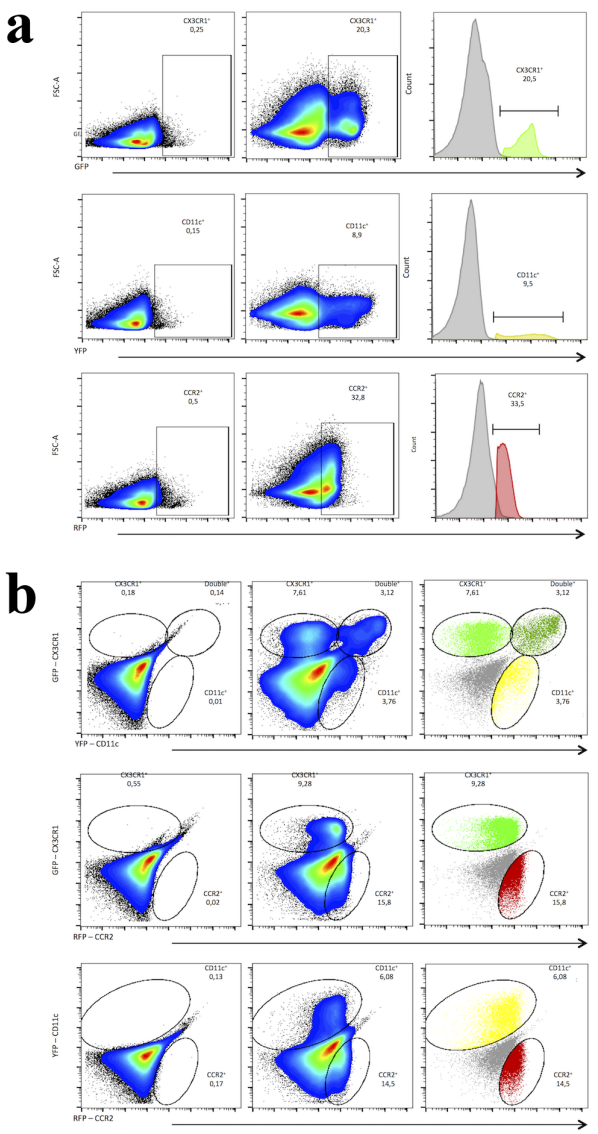

Figure 5 - Efficient flow cytometry separation of liver leucocytes from triple fluorescent mouse CX3CR1$^{gfp/wt}$CCR2$^{rfp/wt}$CD11c-eYFP. (**a**) Individual visualization of GFP fluorescence (FL1 channel – filter 510/15nm), YFP (FL2 – filter 540/20nm) and RFP (FL3 – filter 610/20nm) on Accuri C6 (BD Biosciences) cytometer of triple fluorescent mice compared to WT animals. (**b**) Simultaneous expression of CX3CR1, CD11c and CCR2 evidencing individual populations of each receptor and the presence of double-positive cells for CX3CR1 and CD11c. CCR2+ cell populations do not express CX3CR1 neither CD11c in homeostatic conditions.

INTRAVASCULAR ROUND CCR2+ AND CCR2+CX3CR1+ CELLS RAPIDLY CRAWL AFTER LOCAL INJURY, WHILE EXTRAVASCULAR CELLS REMAINED SESSILE

We next sought to investigate the dynamics of these phagocyte populations under liver injury. For this, we generated a delicate small thermal injury in the liver surface of an anesthetized CX3CR1$^{gfp/wt}$CCR2$^{rfp/wt}$CD11c-eYFP mouse and monitored cell behavior up to three hours. To precisely circumscribe the damaged area, we stained dead cells with DAPI, a fluorescent probe that binds strongly to A-T rich regions in DNA of dead cells. In addition, we taken advantage of a motorized XY stage to

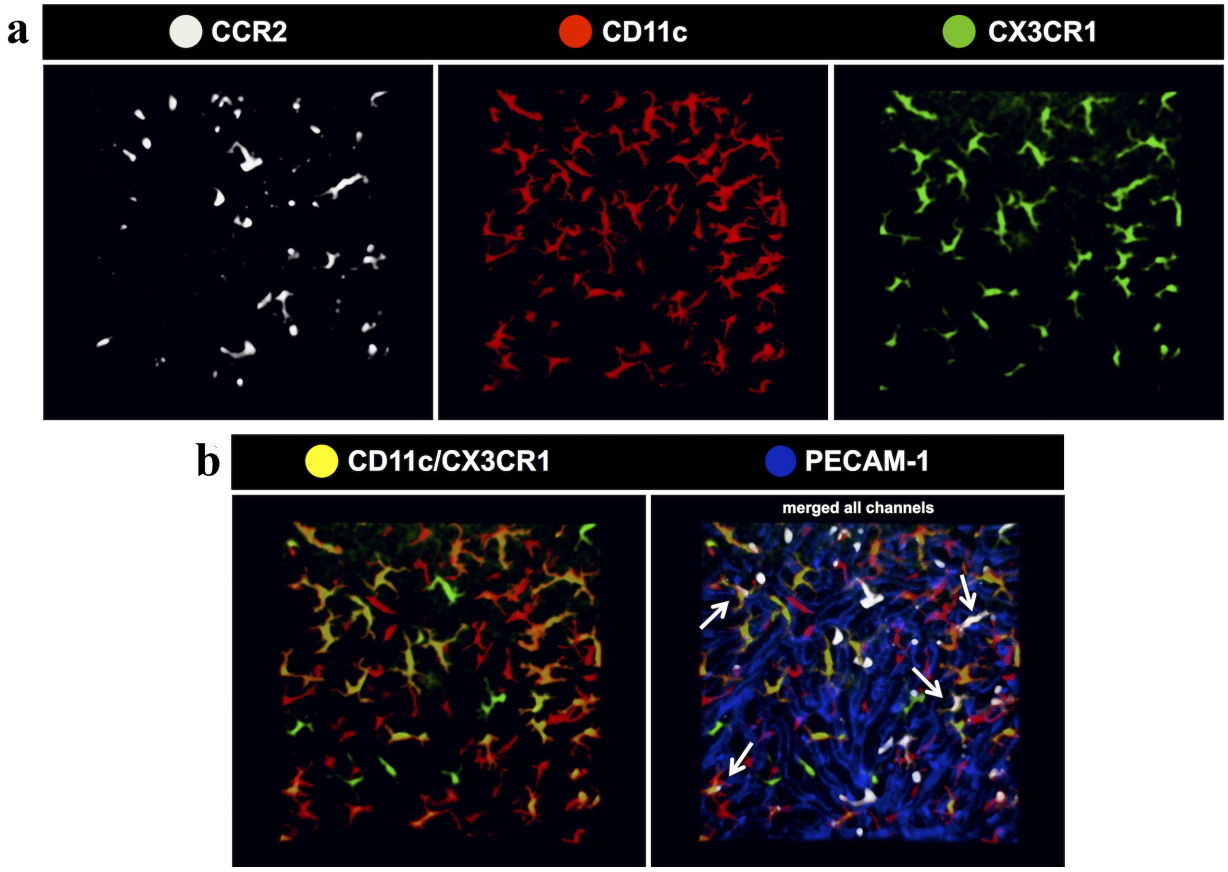

Figure 6 - Efficient spectral separation of liver phagocytes from triple fluorescent mouse CX3CR1$^{gfp/wt}$CCR2$^{rfp/wt}$CD11c-eYFP during confocal intravital microscopy. (**a**) Separated channels from the different populations CCR2+ (white), CD11c+ (red) and CX3CR1+ (green). (**b**) Merged channels showing populations of double-positive cells for CCR2 and CX3CR1 (yellowish cells) and the compartmentalization (intra or extravascular) of cells using PECAM-1. Arrows depict triple positive cells.

simultaneously image three distinct liver regions: the lesion site, the adjacent region close to necrosis and a distant area that was not injured by the thermal probe. To enhance velocity acquisition and capture very fast cell movements, in this setup we imaged as green cells a mixed population of CD11c+ and/or CX3CR1+ cells. As seen in the Fig. 7 and Supplementary Material (Movies 1-3), our injury procedure generated a circular necrotic area that was restricted to a small field of view (~500mm of diameter). At this site, blue cells are mainly necrotic hepatocytes that incorporated circulating DAPI. Also, while extravascular cells remained sessile throughout the whole imaging protocol, we could observe in all imaged fields a fast and random crawling behavior of CCR2+ cells. These cells also adhered and elongated within the liver sinusoidal lumen, and some even migrated to lesion site. Of note, we imaged an infiltrating and rapidly moving population of green, red or yellowish cells, which we suggest that might comprise a mixed population of monocytes and neutrophils. To dissect which of these cells were neutrophils, we counter stained *in vivo* CX3CR1$^{gfp/wt}$CCR2$^{rfp/wt}$CD11c-eYFP mouse with an intravenous injection of allophycocyanine-conjugated anti-Ly6G (Lymphocyte antigen 6 complex locus G6D), a molecule that is specifically expressed in granulocytes. Despite we could not acquire high quality images as those from our triple fluorescence-reporter mouse, in our images

we observed a Ly6G single positive cell population, corresponding to neutrophils (Fig. 8). It was possible to merge channels in order to find the best combination of markers and differentiate the cell populations. The analysis showed that there were not double-positive cells for Ly6G and CCR2 (Fig. 9). Neutrophils were mostly found close to the injury site, and were also fast moving cells. In a broad field of view, regardless the imaging field chosen, the majority of CCR2+ cells were found patrolling the liver microvasculature, suggesting that the even in non-injured sites, these cells may have a surveillance behavior in the hepatic microenvironment.

DISCUSSION

The advent of novel technologies that allow the identification of particular leukocyte phenotypes and even their complete RNA program in a single cell level have tremendously expanded our knowledge not only in the sharp differences between populations that were previously considered as "homogenous", but also have challenged several of our solid concepts in immunology and cell biology (Mass et al. 2016). Now, cells can be identified and classified by the simultaneous presence/absence up to 40 markers using mass cytometry (CyTOF), and can be recovered to further studies using more than 20 fluorescent markers by flow cytometry-based cell sorting (David et al. 2017, Becher et al. 2014, Amir el et al. 2013). The data raised from these studies revealed that the immune system ontogenesis and diversity is far more elaborated than we ever thought. However, despite their unquestionable relevance, in all aforementioned techniques cells need to be extracted out of their native habitat to be analyzed. Therefore, it is expected that this will

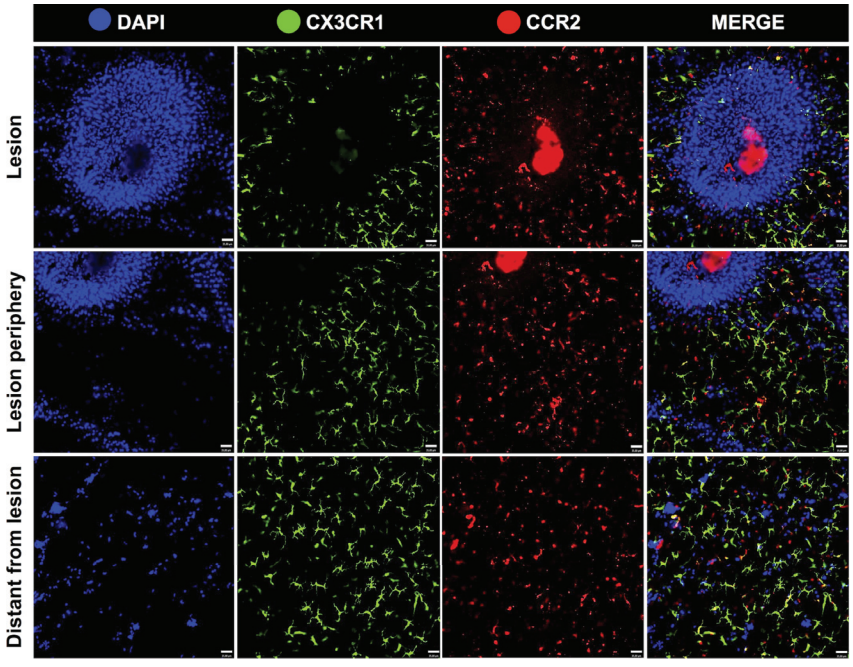

Figure 7 - Dynamics of phagocytic populations under liver injury. Assessing migration dynamics of CX3CR1+ (green) and CCR2+ (red) to three different areas simultaneously using the multi-point imaging feature of Nikon A1R (necrotic zones, areas around necrosis and areas distant from necrosis) by intravital microscopy. A focal thermal necrosis was induced using a hot needle adapted to a cauterizer unit. The hot needle touched the liver surface and resulted on a punctual necrosis, which is delimited with topic DAPI staining (in blue). Scale bars = 35 µm.

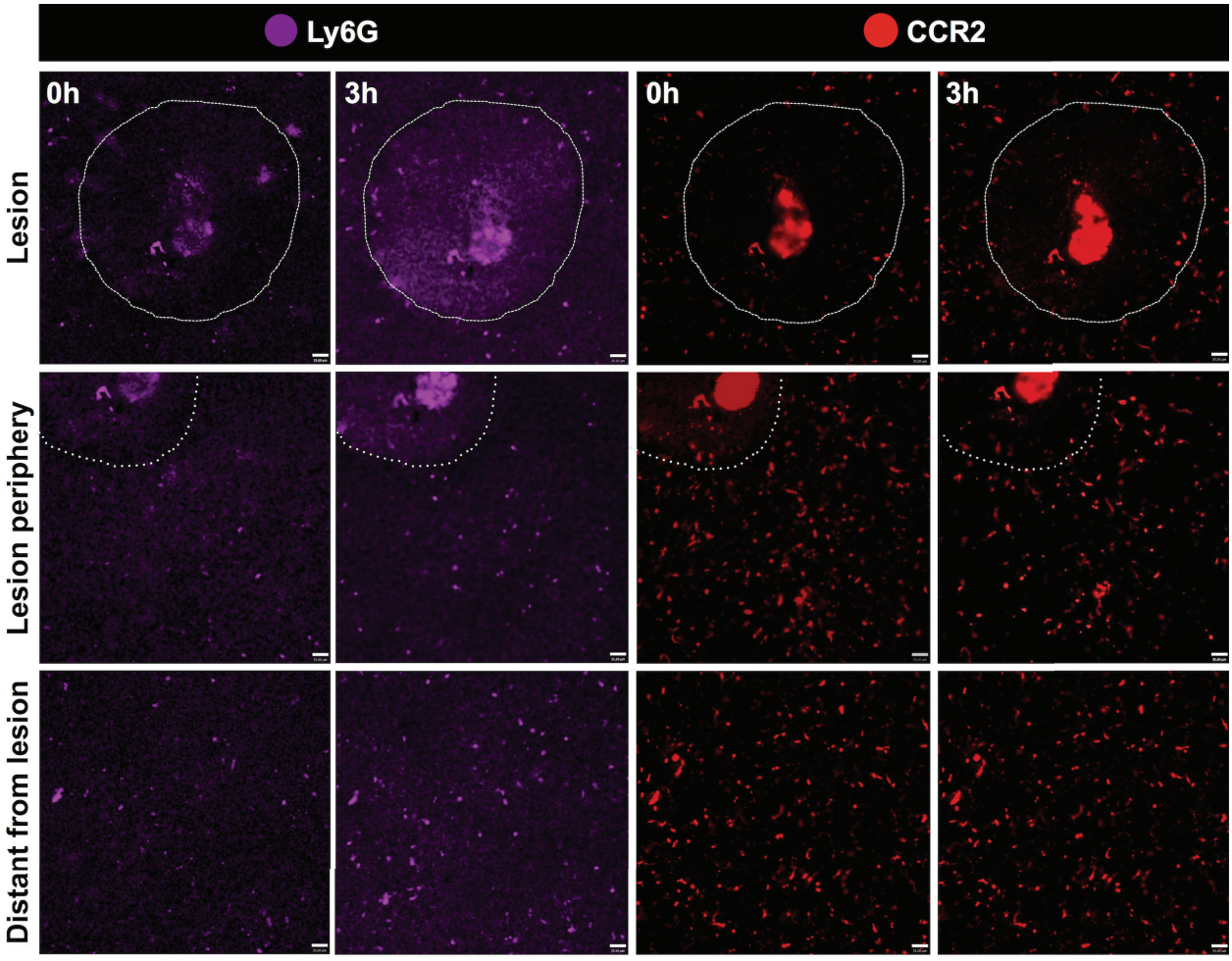

Figure 8 - Dynamics of phagocytic populations under liver injury. Assessing migration dynamics of Ly6G$^+$ (purple) and CCR2$^+$ (red) to necrotic zones, areas around necrosis and areas distant from necrosis using intravital microscopy. Imaging throughout three sequential hours. A hot needle, adapted to a cauterizer unit, induced liver injury. The needle was put on the liver surface and generated a punctual necrosis, which is delimited by the dotted line. Scale bars = 35 µm.

eventually generate caveats that can be relevant in the context of the spatial relationship between these cells *in vivo*, and their actual expression of these markers and even morphology in the pre-isolation condition. In this paper, we aimed to add to these efforts generating a novel mouse strain that spontaneously express *in vivo* three fluorescent molecules that have been repeatedly used in the most part of these high-fidelity studies. Then, some blocking steps, anti-body staining protocols and specially cell isolation procedures are not always necessarily needed, which we expect that facilitate and improve data acquisition.

The choice of the fluorescent molecules to design our breeding strategy to generate this mouse strain was based on two different, but complementary high relevant research lines: immune cell ontogenesis and *in vivo* behavior leukocyte. CX3CR1 is the receptor for the chemokine CX3CL1, also named fracktalkine. Different to other soluble chemokines, CX3CL1 also exist in a membrane-anchored isoform (Poniatowski et al. 2017). In addition to its classical

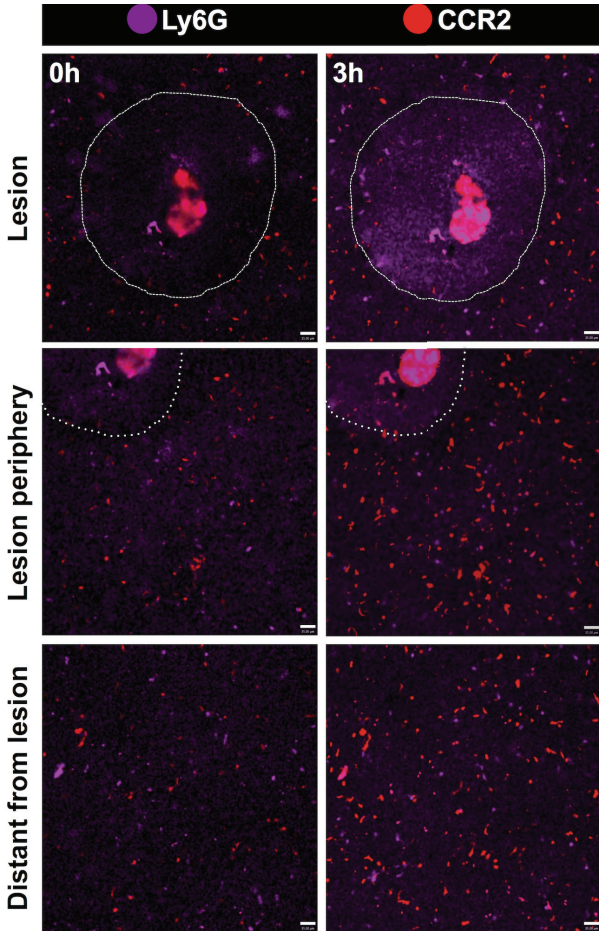

Figure 9 - Dynamics of phagocyte populations under liver injury. Assessing migration dynamics of $Ly6G^+$ (purple) and $CCR2^+$ (red) to necrotic zones, areas around necrosis and areas distant from necrosis using intravital microscopy. Imaging protocol was made throughout three sequential hours. A focal necrosis was induced using a hot needle adapted to a cauterizer unit. The hot needle touched liver surface and generated a punctual necrosis, which is delimited by the dotted line. Neutrophils correspond to $L6yG^+CCR2^+$ cells. Scale bars = 35 µm.

function as a chemoattractant, CX3CR1 has been described in activated endothelial cells, dendritic cells and neurons under homeostasis and disease (Zhou et al. 2016, Zabel et al. 2016). Its high and constant expression in early hematopoietic lineages has fostered landmark studies that have unraveled the origin of both resident macrophages and dendritic cells. In fact, myeloid cells expressing the hematopoietic marker CD45 and the adult macrophage/microglia markers CD11b, F4/80, and CX3CR1 were detectable in the developing brain starting from the embryonic day E9.5 in mice, which reinforce CX3CR1 participation in early states of cell ontogenesis up to adulthood (Ginhoux and Jung 2014). Unfortunately, anti-body based staining of CX3CR1-expressing cells is still under debate in the literature due its low affinity and reliability, making a CX3CR1-reporter mouse strain instrumental to these studies.

Still focusing on the expression of immune-related molecules, the integrin CD11c is constantly present in different leukocytes, and its absence also helps to distinguish different cell population and activation status. CD11c is a surface adhesion molecule that is usually found together with its β-chain CD18 (CD11c/CD18). This complex is the receptor for the complement component iC3b and fibrinogen, and it is also involved in cell adhesion to endothelium. Initially, CD11c was thought to be a specific marker for DCs, which was redefined later in studies showing that CD11c is broadly expressed in several myeloid cells (including macrophages), lymphocytes, natural killer cells and others (Lindquist et al. 2004, David et al. 2016, 2017). We have recently shown using a combination of high-dimensional cell immunophenotying (CyTOF), gene analysis and confocal intravital microscopy that the liver has at least two populations of Kupffer cells that distinctly express CD11c even when they are very similar in shape and are seeded in the same organ compartment (adhered to the sinusoidal lumen). However, a different population of CD11c+ cells was observed in the extravascular space (subcapsular) and is sharply different from the intrasinusoidal Kupffer cells, being bigger in size than Kupffer cells and richer in long dendrites. In these studies, we described these cells as a large population of CD11c+CX3CR1+ expressing DCs (David et al. 2016, 2017). Therefore, either presence or absence of CD11c can be used to distinguish cell populations, and the opportunity

to investigate simultaneously its co-expression with other chemokine receptors, including CCR5, CCR2, and surface molecules including (i.e. CD45 and F4/80) can add substantially in broad-spectrum immunophenotyping studies *in vivo* and *in vitro*.

Still, there has been a particular high interest in investigating the role for CCR2 in leukocyte activation and migration in both homeostasis and diseases. The most studied ligand for CCR2 is the monocyte chemoattractant protein-1 (MCP-1, also known as CCL2). There are two spliced forms of CCR2 that are able to activate different signaling pathways (CCR2A and CCR2B), being CCR2B the mainly isoform expressed by immune cells (~90%) (Bartoli et al. 2001). CCR2 is constitutively expressed in the cell membrane of leukocytes including neutrophils, T cells and monocytes. Of note, CCR2 activation plays a key role in maturation of DCs in different organs (Jimenez et al. 2010). However, under inflammatory conditions, CCR2 mRNA can be upregulated especially due to the release of other chemokines and cytokines, including IL-2, CCL5 and CXCL2, also by non-directly immune-related molecules, including low-density lipoprotein (LDL) (Wiesner et al. 2010). Resident monocytes that traffic into peripheral tissues under homeostatic conditions naturally express low levels of CCR2, but during inflammatory conditions, $CCR2^{hi}$ monocytes instantaneously respond to tissue damage and inflammation. High expression of CCR2, therefore, may be a sign of inflammation, guiding this subset of CCR2+ $Ly6c^{hi}$ monocytes to injured organs. Conversely, $Ly6c^{lo}$ resident monocytes express high levels of CXC3CR1, but not CCR2, making the opportunity to access their simultaneous expression in our novel mouse strain extremely helpful (Mizutani et al. 2012).

CONCLUSIONS

In summary, the novel mouse strain that we generated ($CX3CR1^{gfp/wt}CCR2^{rfp/wt}$CD11c-eYFP) is strategically useful to several studies in immunobiology and other related areas that aim to understand different disease pathogenesis. Indeed, we believe that the opportunity to visualize cells naturally expressing these molecules would essentially add in our understanding of the cell biology under a more untouched condition: their inherent behaviour, their shape, their relationship with other cells and their geographical location *in vivo*.

ACKNOWLEDGMENTS

We would like to thank Maxillofacialtips, BD Biosciences and Nikon for providing reagents, financial and technical support. This work was supported by Fundação de Amparo à Pesquisa do Estado de São Paulo (FAPESP), Fundação de Amparo à Pesquisa do Estado de Minas Gerais (FAPEMIG), Coordenação de Aperfeiçoamento de Pessoal de Nível Superior (CAPES) (Biocomputacional) and Conselho Nacional de Desenvolvimento Científico e Tecnológico (CNPq) (Brazil).

REFERENCES

AMIR EL AD, DAVIS KL, TADMOR MD, SIMONDS EF, LEVINE JH, BENDALL SC, SHENFELD DK, KRISHNASWAMY S, NOLAN GP AND PE'ER D. 2013. viSNE enables visualization of high dimensional single-cell data and reveals phenotypic heterogeneity of leukemia. Nat Biotechnol 31: 545-552.

ARKHIPOV SN, SAYTASHEV I AND DANTUS M. 2016. Intravital Imaging Study on Photodamage Produced by Femtosecond Near Infrared Laser Pulses in vivo. Photochem Photobiol: 92(2): 308-313.

BALMER ML ET AL. 2014. The liver may act as a firewall mediating mutualism between the host and its gut commensal microbiota. Sci Transl Med 6: 237ra266.

BARTOLI C, CIVATTE M, PELLISSIER JF AND FIGARELLA-BRANGER D. 2001. CCR2A and CCR2B, the two isoforms of the monocyte chemoattractant protein-1 receptor are up-regulated and expressed by different cell subsets in idiopathic inflammatory myopathies. Acta Neuropathol 102: 385-392.

BECHER B ET AL. 2014. High-dimensional analysis of the murine myeloid cell system. Nat Immunol 15: 1181-1189.

CRISPE IN. 2009. The liver as a lymphoid organ. Ann Rev Immunol 27: 147-163.

DAVID BA ET AL. 2016. Combination of Mass Cytometry and Imaging Analysis Reveals Origin, Location, and Functional Repopulation of Liver Myeloid Cells in Mice. Gastroenterol 151: 1176-1191.

DAVID BA, RUBINO S, MOREIRA TG, FREITAS-LOPES MA, ARAUJO AM, PAUL NE, REZENDE RM AND MENEZES GB. 2017. Isolation and high-dimensional phenotyping of gastrointestinal immune cells. Immunol 151: 56-70.

DAVIES LC, JENKINS SJ, ALLEN JE AND TAYLOR PR. 2013. Tissue-resident macrophages. Nat Immunol 14: 986-995.

FAUST N, VARAS F, KELLY LM, HECK S AND GRAF T. 2000. Insertion of enhanced green fluorescent protein into the lysozyme gene creates mice with green fluorescent granulocytes and macrophages. Blood 96: 719-726.

FOGG DK, SIBON C, MILED C, JUNG S, AUCOUTURIER P, LITTMAN DR, CUMANO A AND GEISSMANN F. 2006. A clonogenic bone marrow progenitor specific for macrophages and dendritic cells. Science 311: 83-87.

GEISSMANN F, MANZ MG, JUNG S, SIEWEKE MH, MERAD M AND LEY K. 2010. Development of monocytes, macrophages, and dendritic cells. Science 327: 656-661.

GINHOUX F AND JUNG S. 2014. Monocytes and macrophages: developmental pathways and tissue homeostasis. Nat Rev Immunol 14: 392-404.

GOMEZ PERDIGUERO E ET AL. 2015. Tissue-resident macrophages originate from yolk-sac-derived erythro-myeloid progenitors. Nature 518: 547-551.

JENNE CN AND KUBES P. 2013. Immune surveillance by the liver. Nat Immunol 14: 996-1006.

JIMENEZ F, QUINONES MP, MARTINEZ HG, ESTRADA CA, CLARK K, GARAVITO E, IBARRA J, MELBY PC AND AHUJA SS. 2010. CCR2 plays a critical role in dendritic cell maturation: possible role of CCL2 and NF-kappa B. J Immunol 184: 5571-5581.

KARREMAN MA, HYENNE V, SCHWAB Y AND GOETZ JG. 2016. Intravital Correlative Microscopy: Imaging Life at the Nanoscale. Trends Cell Biol 26: 848-863.

LINDQUIST RL, SHAKHAR G, DUDZIAK D, WARDEMANN H, EISENREICH T, DUSTIN ML AND NUSSENZWEIG MC. 2004. Visualizing dendritic cell networks in vivo. Nat Immunol 5: 1243-1250.

MARQUES PE, ANTUNES MM, DAVID BA, PEREIRA RV, TEIXEIRA MM AND MENEZES GB. 2015. Imaging liver biology in vivo using conventional confocal microscopy. Nat Protoc 10: 258-268.

MASS E ET AL. 2016. Specification of tissue-resident macrophages during organogenesis. Science 353(6304): aaf4238.

MCDONALD B, PITTMAN K, MENEZES GB, HIROTA SA, SLABA I, WATERHOUSE CC, BECK PL, MURUVE DA AND KUBES P. 2010. Intravascular danger signals guide neutrophils to sites of sterile inflammation. Science 330: 362-366.

MIZUTANI M, PINO PA, SAEDERUP N, CHARO IF, RANSOHOFF RM AND CARDONA AE. 2012. The fractalkine receptor but not CCR2 is present on microglia from embryonic development throughout adulthood. J Immunol 188: 29-36.

PARKHURST CN, YANG G, NINAN I, SAVAS JN, YATES JR, 3RD, LAFAILLE JJ, HEMPSTEAD BL, LITTMAN DR AND GAN WB. 2013. Microglia promote learning-dependent synapse formation through brain-derived neurotrophic factor. Cell 155: 1596-1609.

PONIATOWSKI LA, WOJDASIEWICZ P, KRAWCZYK M, SZUKIEWICZ D, GASIK R, KUBASZEWSKI L AND KURKOWSKA-JASTRZEBSKA I. 2017. Analysis of the Role of CX3CL1 (Fractalkine) and Its Receptor CX3CR1 in Traumatic Brain and Spinal Cord Injury: Insight into Recent Advances in Actions of Neurochemokine Agents. Mol Neurobiol 54: 2167-2188.

THOMSON AW AND KNOLLE PA. 2010. Antigen-presenting cell function in the tolerogenic liver environment. Nat Rev Immunol 10: 753-766.

WIESNER P ET AL. 2010. Low doses of lipopolysaccharide and minimally oxidized low-density lipoprotein cooperatively activate macrophages via nuclear factor kappa B and activator protein-1: possible mechanism for acceleration of atherosclerosis by subclinical endotoxemia. Circ Res 107: 56-65.

YIPP BG ET AL. 2012. Infection-induced NETosis is a dynamic process involving neutrophil multitasking in vivo. Nat Med 18: 1386-1393.

YONA S ET AL. 2013. Fate mapping reveals origins and dynamics of monocytes and tissue macrophages under homeostasis. Immunity 38: 79-91.

ZABEL MK, ZHAO L, ZHANG Y, GONZALEZ SR, MA W, WANG X, FARISS RN AND WONG WT. 2016. Microglial phagocytosis and activation underlying photoreceptor degeneration is regulated by CX3CL1-CX3CR1 signaling in a mouse model of retinitis pigmentosa. Glia 64: 1479-1491.

ZHOU B, XU H, NI K, NI X AND SHEN J. 2016. Expression of Chemokine XCL2 and CX3CL1 in Lung Cancer. Med Sci Monit 22: 1560-1565.

SUPPLEMENTARY MATERIAL

Supplementary Movie 1 - Distant from lesion area - Liver confocal intravital microscopy showing in green $CX3CR1^+$/$CD11c^+$ cells, in red $CCR2^+$ cells and necrotic cells in blue (DAPI). Imaging protocol was made throughout three sequential hours. A focal necrosis was induced using a hot needle adapted to a cauterizer unit. The hot needle touched liver surface and generated a punctual necrosis, which is delimited by the dotted line. These three movies were acquired simultaneously *in vivo* using the multi-point (XYZ) motorized stage at Nikon A1R (necrotic zones, areas around necrosis and areas distant from necrosis).

Supplementary Movie 2 - Periphery of lesion - Liver confocal intravital microscopy showing in green $CX3CR1^+$/$CD11c^+$ cells, in red $CCR2^+$ cells and necrotic cells in blue (DAPI). Imaging protocol was made throughout three sequential hours. A focal necrosis was induced using a hot needle adapted to a cauterizer unit. The hot needle touched liver surface and generated a punctual necrosis, which is delimited by the dotted line. These three movies were acquired simultaneously *in vivo* using the multi-point (XYZ) motorized stage at Nikon A1R (necrotic zones, areas around necrosis and areas distant from necrosis).

Supplemental Movie 3 - Lesion area - Liver confocal intravital microscopy showing in green $CX3CR1^+$/$CD11c^+$ cells, in red $CCR2^+$ cells and necrotic cells in blue (DAPI). Imaging protocol was made throughout three sequential hours. A focal necrosis was induced using a hot needle adapted to a cauterizer unit. The hot needle touched liver surface and generated a punctual necrosis, which is delimited by the dotted line. These three movies were acquired simultaneously *in vivo* using the multi-point (XYZ) motorized stage at Nikon A1R (necrotic zones, areas around necrosis and areas distant from necrosis).